Indoor Office Propagation Measurements and Path Loss Models at 5.25 GHz

Ding Xu*, Jianhua Zhang*, Xinying Gao*, Ping Zhang* and Yufei Wu†
*Key Laboratory of Universal Wireless Communication, Ministry of Education,
Beijing University of Posts and Telecommunications, Beijing 100876, China
†Motorola Ltd., Illinois 60196, America

***Abstract*—Based on 5.25 GHz wideband channel measurements performed in indoor office environment, empirical path loss models in in-room line-of-sight (LoS), room-corridor, and room-room non-line-of-sight (NLoS) propagation conditions are developed for future wireless radio systems. One-slope and dual-slope log-distance models are adopted in in-room LoS and room-corridor conditions, respectively. In room-room NLoS condition, we propose the enhanced attenuation factor models: AF-extended and AF-linear models to further explore the effect of medium walls, heavy walls and doors. This work offers valuable propagation measurements in a frequency range that is being considered allocating to IMT-Advanced systems.**

***Index Terms*—5.25 GHz, wideband channel measurements, path loss models, attenuation factor, IMT-Advanced systems**

I. Introduction

Path loss models are important for coverage prediction and interference analysis in simulation and design of wireless communication systems. Recently much research work has been devoted to the development of IMT-Advanced systems [1]. Due to narrower spectrum bands available below 3 GHz, IMT-Advanced systems are most likely to utilize considerably higher carrier frequencies up to 5 GHz. Several publications have existed for indoor path loss models at 5 GHz [2]–[5], but they are all using the simple one-slope log-distance models in non-line-of-sight (NLoS) condition.

In this paper, empirical indoor office path loss models at 5.25 GHz are presented based on an extensive set of experimental data collected in an office building in Beijing, China. The measurements covers in-room line-of-sight (LoS), room-corridor, and room-room NLoS propagation conditions. In-room LoS denotes transmitter (TX) and receiver (RX) are in the same room in LoS condition; room-corridor denotes TX is fixed in room and RX is in the corridor; room-room NLoS denotes TX and RX are in different rooms in NLoS condition. Traditional one-slope log-distance model is presented in in-room LoS condition, while dual-slope log-distance model is proposed in room-corridor condition. In room-room NLoS condition, log-distance, Devasirvatham, and three different attenuation factor models are evaluated. The AF-Extended model and AF-Linear model are proposed for lower estimation error compared to other models.

The research is funded by China National 863 Project: Wideband MIMO channel modeling and simulation in the next generation network (No. 2006AA01Z258), the 111 project (No. B07005) and Motorola Ltd.

This paper is organized as follows. Section II presents the radio channel measurement equipment and describes the measurement environment. Section III describes the post-processing approach and introduces different path loss models. Section IV presents analysis of the measurement results and path loss models. Section V gives the conclusions of this work.

II. Measurement Description

Radio channel measurements were performed with 100 MHz bandwidth at 5.25 GHz center frequency by using PropSound (TM), Elektrobit multidimensional radio channel sounder [6]. The 3D cylindrical omni-directional array (ODA) with 25 dual-polarized patch elements shown in Fig. 1(a) is used at the TX, while the vertically polarized uniform circular array (UCA) with 7+1 monopoles in Fig. 1(b) is used at the RX. The transmit power is 26 dBm. Summary of measurement parameters is given in Table I.

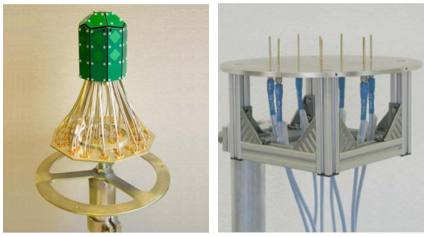

(a) 2x9 ODA (b) 7+1 UCA

Fig. 1. TX and RX antenna arrays

TABLE I
Measurement Parameters

Carrier frequency [GHz]	5.25
Bandwidth [MHz]	100
Chip rate [MHz]	100
Transmit power [dBm]	26
Code length [μs]	5.11
Cycle rate [Hz]	21.7
Number of TX elements	50
Number of RX elements	8
TX antenna height [m]	2.5
RX antenna height [m]	1.5

The measurements were performed on the third floor of a typical modern three-story office building built in 2004. The

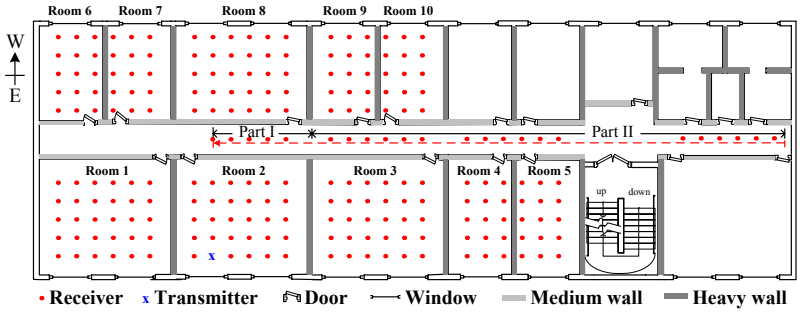

Fig. 2. Floor plan and TX and RX locations

floor plan and TX and RX locations for the measurement campaign are shown in Fig. 2. The floors and walls are made of reinforced concrete, and two types of walls are existed in the building, i.e. medium wall (thickness of 20 cm) and heavy wall (thickness of 30 cm). Throughout the building the windows are single glazed with clear window glass. The office doors are made of clear glass with thickness of 10 mm. During the measurements, all doors except room 2's were closed. The corridor is 37.0-m-long, 1.6-m-wide and 2.5-m-high. The ceiling height of every room is 4 m. On the west side of the corridor, the dimensions of small and large rooms are 5 m $\times$ 3.5 m and 5 m $\times$ 7 m. On the east side of the corridor, the dimensions of small and large rooms are 6 m $\times$ 3.5 m and 6 m $\times$ 7 m. We consider this floor to be a reasonable representation of office environment.

During measurements, TX was fixed stationary 2.5 m above the floor in room 2. The dots in Fig. 2 denote RX stationary measurement locations. The dashed line denotes RX pedestrian measurement route in corridor. For each stationary measurement location, 100 snapshots of channel responses were recorded for post processing. The inverse of time duration between two snapshots is denoted as cycle rate, which is 21.7 Hz in both stationary and low mobility measurements.

III. Path Loss Models

We define path loss as the ratio of the effective transmitted power to the received power, calibrating out cable losses, amplifier gains, and antenna gains. In order to filter out the effect of fast fading and suppress the noise fluctuation, local power delay profile (PDP) is derived by averaging the received power over the 50$\times$8 sub-channels for each snapshot of channel response. Additionally, time averaging in 20 PDPs and spatial averaging over a window of 20 λ (λ is the wavelength) are performed at each stationary measurement location and pedestrian measurement track in corridor, respectively [7]. As a result, five averaged local PDPs are obtained at each stationary measurement location, and totally 29 averaged local PDPs are obtained in corridor pedestrian measurement. After that, dynamic range is set at -18 dB in the delay domain relative to the strongest multipath to cut the noise [8]. The averaged local PDPs are discarded if not satisfy the dynamic range. Then, measured path loss can be calculated as [9]

$$PL = -10\ \log_{10}(\sum_{\tau} P_\tau) \tag{1}$$

where P_τ is the averaged local PDPs at a certain delay τ.

Free space loss between TX and RX, assuming isotropic antennas located in a perfectly dielectric, homogeneous, and unlimited environment, is given by [10]

$$PL_{fs}(d) = 20\ \log_{10}(\frac{4\pi d}{\lambda}) \tag{2}$$

where d is the TX-RX separation distance in meters.

The commonly used one-slope log-distance model is [11]–[13]

$$PL_{ld}(d) = A + 10n\ \log_{10}(d) \tag{3}$$

where A denotes the path loss intercept, n is the path loss exponent which describes how fast the path loss increases with distance. The model parameters to be fitted are A and n.

The traditional attenuation factor model is given by free space loss added with attenuation factor [11]

$$\begin{aligned} PL_{AF}(d) &= PL_{fs}(d) + A_F \\ &= 20\ \log_{10}(\frac{4\pi d}{\lambda}) + A_F \end{aligned} \tag{4}$$

where A_F is the attenuation factor, in our measurements, expressed as

$$A_F = i\,L_{w1} + j\,L_{w2} + k\,L_d \tag{5}$$

where L_{w1}, L_{w2} and L_d are the attenuation factors due to traversed partitions, i.e. heavy wall, medium wall and glass door; i, j and k are the corresponding number, respectively. The parameters to be fitted are L_{w1}, L_{w2}, and L_d. We refer to this model as AF-Classic (AFC). A more complicated attenuation factor model is the extension of AFC, which assumes the loss between traversed partitions is not in free space, expressed as (3) added with A_F, i.e.

$$\begin{aligned} PL_{AF}(d) &= PL_{ld}(d) + A_F \\ &= A + 10n\ \log_{10}(d) + A_F. \end{aligned} \tag{6}$$

This second attenuation factor model is referred to as AF-Extended (AFE). This model's parameters to be fitted are A, n, L_{w1}, L_{w2} and L_d.

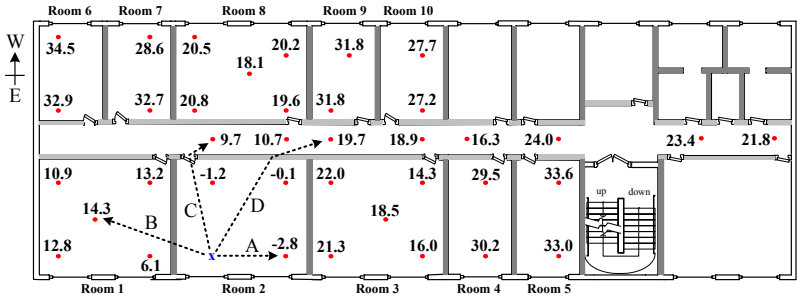

Fig. 3. Example of measured excess path loss and four propagation mechanisms A–D

The third attenuation factor model considered in this paper is the modification of the model proposed by Devasirvatham in [14]. Devasirvatham found that the indoor path loss obeys free space loss plus an additional loss factor increasing linearly with TX-RX separation distance i.e. $PL_{fs}(d) + \alpha$, where α is the attenuation constant with units of dB per meter (dB/m). Adding the attenuation factor A_F, we modify the model in [14] as follows

$$\begin{aligned} PL_{AF}(d) &= PL_{fs}(d) + \alpha\, d + A_F \\ &= 20\, \log_{10}(\frac{4\pi d}{\lambda}) + \alpha\, d + A_F. \end{aligned} \tag{7}$$

We refer to this model as AF-Linear (AFL). The parameters to be fitted are α, L_{w1}, L_{w2} and L_d. Compared with AFC, AFL adds the parameter α to revise the loss between partitions.

The parameters of above path loss models are determined through regression analysis using the least-square (LS) method.

IV. Measurement Results

In indoor environment, the main propagation mechanisms are propagation through LoS path (A), propagating through walls (B), diffraction through doorway (C), and diffuse scattering from the non-homogeneous walls (D), as illustrated in Fig. 3. Mechanism A is only existed in LoS condition. Mechanism B depends on the construction materials, thickness of walls and number of traversed walls. Mechanism C is mainly occurred when radio waves propagate out of or into the rooms. Mechanism D is caused by the impurity of the construction materials (e.g. the supporting structures in walls). It should be noticed that the propagation mechanisms are combined together in most propagation conditions. Fig. 3 also shows some example of the measured path loss relative to free space loss, which we denotes as excess path loss. The negative values in Fig. 3 indicate losses lower than in free space. In the following subsection, detailed propagation characteristics as well as path loss models are presented.

A. In-room LoS

From Fig. 3 it is noticeable that the measurements taken in LoS in room 2 are the only ones to show path loss lower than free space loss. Besides propagation mechanism A, reflected and scattered multipath by surrounding objects, e.g. walls, floor, ceiling, and office desks, contribute to received energy. In such case the path loss is lower than free space loss.

The plot of measured path loss along with LS fitting of one-slope log-distance model is shown in Fig. 4(a). The model is as follows

$$PL(d) = 47.8 + 14.8 \log_{10}(d),\ \sigma = 1.3\, dB \tag{8}$$

where the path loss exponent is 1.48, smaller than free space exponent 2, which implies a guided wave phenomenon due to walls, floor, and ceiling of the room, as observed in literature [2]–[4]; σ is the standard deviation of the estimation error, which is frequently modeled as a zero mean Gaussian variable.

B. Room-corridor

In this propagation condition, both stationary and pedestrian measurements were conducted in this scenario. Obtained path loss from two measurements are put together for analysis. Propagation mechanism B, C, and D are dominating the radio propagation in this environment. Due to the high attenuation introduced by multiple walls, the waveguide effect in the corridor is much stronger at the corridor part II in Fig. 2 than the locations adjacent to room 2 (part I), and there will be a loss passing from part I to part II. This fact is confirmed from Fig. 3 where the excess path loss in part I is clearly lower than part II.

As discussed above, the so-called dual-slope log-distance model is utilized. First the measured path loss data is separated into two parts, then the path loss obtained from the measurement part I is used to get the first slope model, and the data obtained from the measurement part II is used to get the second slope model. The plot of the measured path loss along with the dual-slope log-distance model is shown in Fig. 4(b). The model is given by

$$PL(d) = \begin{cases} 53.2 + 25.8 \log_{10}(d) & d \le d_1 \\ 56.4 + 29.1 \log_{10}(d) & d > d_1 \end{cases},\ \sigma = 1.9\, dB \tag{9}$$

where d_1 is the break point distance of two parts. In the measurements, d_1 equals to about 9 m.

Finally, if a rule-of-thumb is needed to get a quick estimate of path loss, following one-slope log-distance model which is

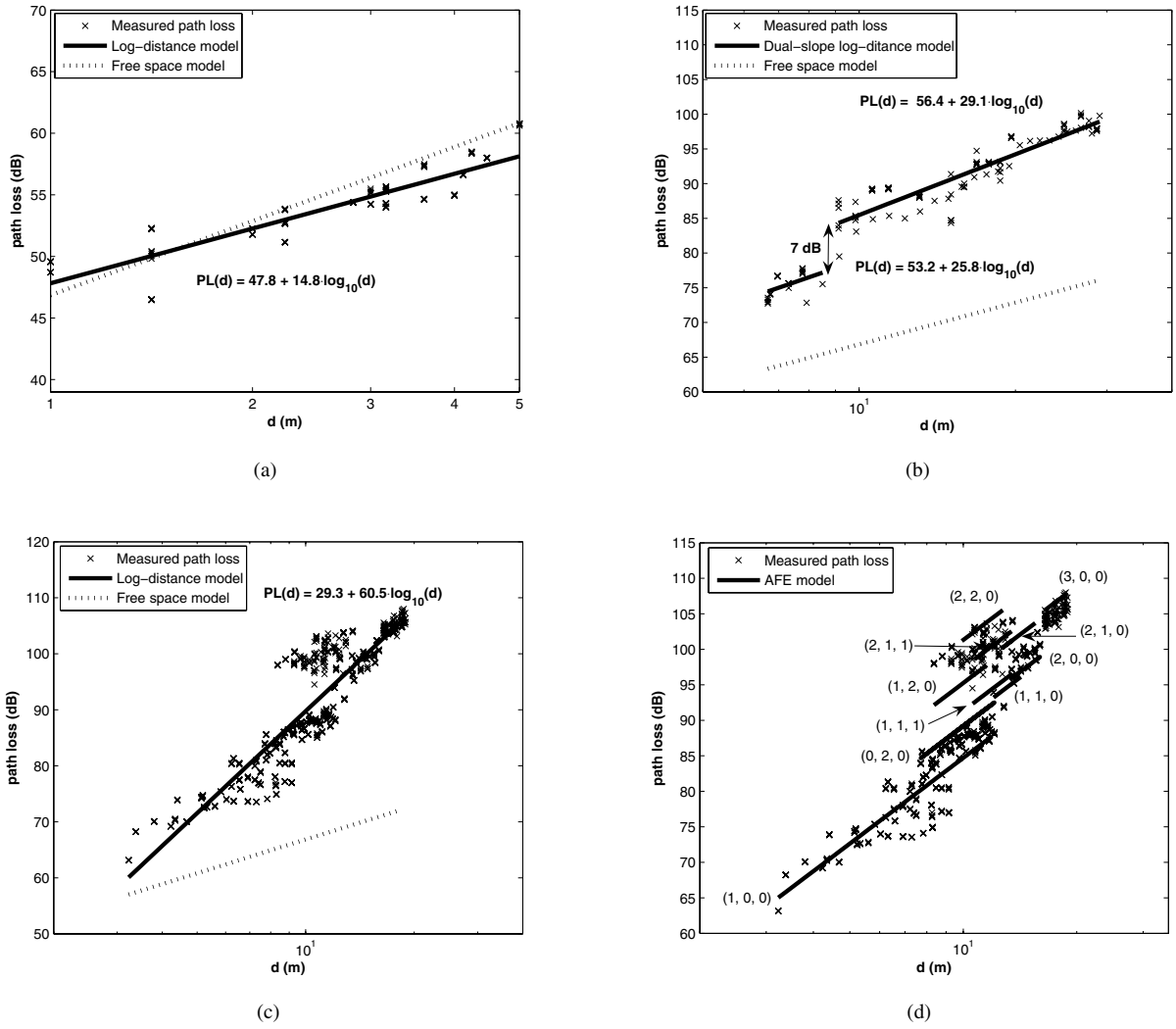

Fig. 4. Measured path loss and models (a) one-slope log-distance model in in-room LoS condition (b) dual-slope log-distance model in room-corridor condition (c) one-slope log-distance model in room-room NLoS condition (d) AFE model in room-room NLoS condition.

obtained by LS fitting of all measured path loss, is proposed

$$PL(d) = 41.9 + 41.0\log_{10}(d),\ \sigma = 2.8\,dB \qquad (10)$$

where the standard deviation of the estimation error is 2.8 dB, which is larger than the corresponding value in (9).

C. Room-room NLoS

In this propagation condition, several rooms were measured, i.e. room 1 and room 3–10. Propagation mechanisms are complicated, e.g., from Fig. 3 it can be observed that the excess path loss in room 1 is lower than in room 3 although both rooms are blocked by one heavy wall from TX; in room 3 the excess path loss near the door is smaller than the other part; the excess path loss in room 8 is similar to room 3 although there are two medium walls blocked TX and RX in room 8. The strong propagation mechanism C combined with waveguide in the corridor contributes significantly to the signal power in these situations. Considering the complicated propagation, we did not separate the data but put all measured path loss in rooms together to do the regression analysis.

Fig. 4(c) and Fig. 4(d) show the path loss obtained from log-distance model and AFE along with measured path loss. The values of (i, j, k) are also shown in Fig. 4(d). Different from log-distance model, the attenuation factor models might generate more than one path loss at the same TX-RX separation distance as in Fig. 4(d). In the real indoor environment, path loss may be large different at the same TX-RX separation distance but different locations, as can be seen in Fig. 3. So, attenuation factor models are more appropriate than log-distance model from this aspect.

Table II shows the LS fitting parameters of log-distance and attenuation factor models. The optimal parameter for Devasirvatham model is also listed. It can be observed from Table II that the attenuation factor due to glass door is important and can not be neglected. It is important to notice that the attenuation factors in Table II are not the physical wall loss

TABLE II
PATH LOSS MODELS PARAMETERS

Models	A	n	L_{w1}	L_{w2}	L_d	α	σ
Log-distance	29.3	6.05	–	–	–	–	4.9
Devasirvatham	–	–	–	–	–	2.1	5.1
AFC	–	–	12.6	9.9	2.3	–	4.6
AFE	38.5	4.01	6.1	5.3	1.4	–	3.2
AFL	–	–	5.5	5.3	1.8	1.2	3.4

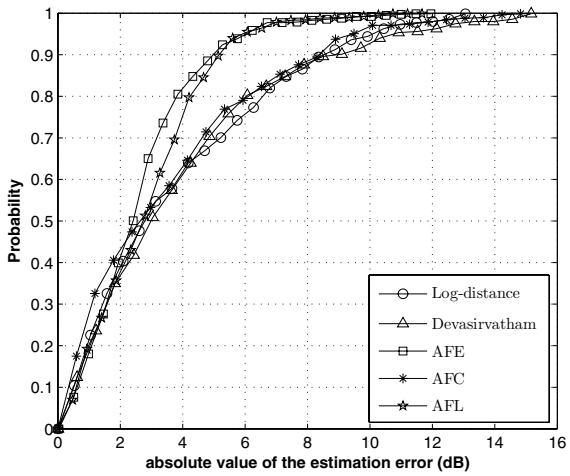

Fig. 5. Cumulative distribution function of the absolute estimation error

and door loss but model parameters which are optimized along with the measured path loss data using regression analysis. In other words, the attenuation factors implicitly include the effect of multipath, etc. To make this clear, the physical wall loss using a 5 ns time window size based on inspection of samples of measurements is also calculate, as in [15]. The result of physical wall loss is 0.82 dB/cm, which is similar with the value presented in [16].

In order to compare the goodness of selected models, standard deviation of estimation error (σ) is also listed in Table II. It can be seen that AFE and AFL yield lower estimation error than other three models. This fact is further demonstrated from the cumulative distribution function of the absolute estimation error in Fig. 5. It can be observed that the 90% of estimated loss are within an absolute estimation error not greater than 5 dB and 5.5 dB for AFE and AFL, respectively. For the log-distance, Devasirvatham and AFC models the previous limit is increased to about 8.5 dB. As expected, non negligible improvement is observed when extending from AFC to AFE and to AFL.

From the analysis above, the AFE and AFL are recommended for modeling the path loss in room-room NLoS propagation condition.

V. Conclusion

This paper has presented the results of path loss measurement campaign conducted in a modern office building at 5.25 GHz carrier frequency. Empirical indoor office path loss models are presented in three different propagation conditions, i.e. in-room LoS, room-corridor, and room-room NLoS.

From measurements, one-slope log-distance model is proposed to describe path loss variation with distance in in-room LoS condition. The result of path loss exponent is 1.48, which is smaller than 2, implying a guided wave phenomenon due to walls, floor, and ceiling of the room. In room-corridor propagation condition, dual-slope log-distance model is proposed to accurately model path loss. If need to get a quick estimate of path loss, one-slope log-distance model is also presented. In room-room NLoS propagation condition, log-distance, Devasirvatham, and attenuation factor models are compared based on estimation error. Apart from attenuation factors introduced from medium walls and heavy walls, we include attenuation factor due to doors in attenuation factor models. Performance improvements are observed when passing from the AFC to the enhanced attenuation factor models AFE and to the AFL. As a result, AFE and AFL are proposed for noticeably lower estimation error.

Acknowledgment

The authors would like to thank the engineers of Elektrobit company, Finland, for their efforts in the measurement campaign.

References

[1] ITU-R M.[IMT.NAME], "Naming for international mobile telecommunications," draft new recommendation.
[2] J. Kivinen, X. Zhao, and P. Vainikainen, "Empirical characterization of wideband indoor radio channel at 5.3 GHz," *IEEE Trans. Antennas Propag.*, vol. 49, no. 8, pp. 1192–1203, Aug. 2001.
[3] K.-G. Tan and S. Denno, "Empirical characterisation of indoor broadband propagation channel," in *Proc. IEEE PIMRC '03*, vol. 1, Sep. 2003, pp. 950–954.
[4] J. Medbo and J. Berg, "Simple and accurate path loss modeling at 5 GHz in indoor environments with corridors," in *Proc. IEEE VTC '00*, Sep. 2000, pp. 30–36.
[5] J. T. E. McDonnell, "5 GHz indoor channel characterization: measurements and models," in *Proc. IEE Antennas and Propagation for Future Mobile Communications Colloquium*, Feb. 1998, pp. 10/1–10/6.
[6] *Propsound multidimensional channel sounder*, Elektrobit Ltd. [Online]. Available: http://www.propsim.com
[7] T. S. Rappaport, "characterization of UHF multipath radio channels in factory buildings," *IEEE Trans. Antennas Propag.*, vol. 37, no. 8, pp. 1058–1069, Aug. 1989.
[8] ITU-R P.1407, "Multipath propagation and parameterization of its characteristics."
[9] ITU-R P.341, "The concept of transmission loss for radio links."
[10] ITU-R PN.525, "Calculation of free-space attenuation."
[11] S. Y. Seidel and T. S. Rappapat, "914 MHz path loss pradiction models for indoor wimless communications in multi-floored buildings," *IEEE Trans. Antennas Propag.*, vol. 40, pp. 207–217, Feb. 1992.
[12] D. Molkdar, "Review on radio propagation into and within buildings," *IEE Proceedings-H Microwaves, Antennas and Propagation*, vol. 138, no. 1, pp. 61–73, Feb. 1991.
[13] H. Hashemi, "The indoor radio propagation channel," *Proc. IEEE*, vol. 81, no. 7, pp. 943–968, Jul. 1993.
[14] D. M. J. Devasirvatham, C. Banerjee, M. Krain, and D. Rappaport, "Multi-frequency radiowave propagation measurements in the portable radio environment," in *Proc. IEEE ICC '90*, Apr. 1990, pp. 1334–1340.
[15] D. Cheung and C. Prettie, "A path loss comparison between the 5 GHz UNII band (802.11a) and the 2.4 GHz ISM band (802.11b)," Intel Labs, Tech. Rep., Jan. 2002.
[16] Y. Zhang and Y. Hwang, "Measurements of the characteristics of indoor penetration loss," in *Proc. IEEE VTC '94*, vol. 3, Jun. 1994, pp. 1741–1744.